Proceedings World Geothermal Congress 2010
Bali, Indonesia, 25-29 April 2010

Advanced Technique for Reservoir Thermal Properties Determination and Pore Space Characterization

Yuri Popov[1], Dmitriy Miklashevskiy[1], Raisa Romushkevich[1], Sergey Safonov[2], Sergey Novikov[1]

1 - Russian State Geological Prospecting University, Miklukho-Maklai str., 23, Moscow 117997

2 - Sclumberger Moscow Research, Ogorodnaya Sloboda 5A, Moscow 101000

yupopov@dol.ru

Keywords: thermal properties, rocks, measurements, equipment, methods

ABSTRACT

New research complex including experimental and theoretical base is developed for simultaneous determination of thermal conductivity, thermal diffusivity and volumetric heat capacity of dense and highly porous and fractured rocks at normal and formation thermodynamical conditions. Experimental base includes (1) a set of non-destructive contactless high precision optical scanning instruments for determination of rock's thermal properties accounting for anisotropy and inhomogeneity, (2) instruments for measurements of rock's thermal properties at simultaneous influence of elevated temperature and porous pressure and two component overburden pressure, (3) instrument for fluid thermal conductivity measurements, (4) extended database on rock thermal properties and their correlations with reservoir and other physical properties established from numerous measurements on representative core collections. Theoretical base consists of new theoretical models of effective thermal properties that allow us (1) to predict rock's thermal properties at normal and elevated temperatures and pressures from other petrophysical data, (2) to estimate reservoir properties, pore fracturing and pore space parameters from thermal physical experiments. The new technique presents qualitatively new possibilities for geothermal research and industrial goals.

1. INTRODUCTION

Data on the thermal properties of rocks such as thermal conductivity, thermal diffusivity, volumetric heat capacity and coefficient of linear thermal expansion are important for many goals in applied and basic geophysics: (1) interpretation of temperature logging data, (2) theoretical modeling heat and mass transfer in formations, (3) determination of heat flow density and its distribution along wells and interpretation of its vertical variations, (4) prediction of other formation's physical properties from the correlations found between thermal and other physical properties. In geothermal energy industry the thermal properties are especially important since they influence essentially on economical aspects of geothermal energy production. Increasing necessity in thermal property data stimulated the development of new effective approaches and equipment to provide more reliable and detailed information about rock's thermal properties.

Recently, advances in determining the thermal properties from the measurements in wells have been made through the development thermal relaxation methods (Wilhelm, 1990), and various types of logging tools (Williams and Anderson, 1990; Burkhardt et al., 1990; Pribnow et al., 1993; Kukkonen et al., 2007). While valuable to specialized applications and important for interpolation between widely spaced samples, these approaches are no substitutes for laboratory measurements on rock samples when cores and cuttings are available.

In spite of numerous instruments for the laboratory measurements of rock thermal properties have been developed during many previous years, the following unsolved problems did not allow to obtain representative and reliable information on the rock thermal properties especially for reservoirs: (1) disturbing influence of the thermal resistance of a sample-equipment contact on the measurement results particularly for porous and fractured rocks, (2) not satisfactory metrological parameters (with the accuracy + precision value more than 7-8% in most cases), (3) significant influence of rock inhomogeneity and anisotropy which could not be accounted most often, (4) impossibility to measure thermal conductivity and thermal diffusivity tensor components simultaneously in most cases, (5) impossibility to provide the non-destructive measurements on full cores and core plugs, (6) absence of instruments for the simultaneous measurements of thermal conductivity and thermal diffusivity tensor components at simultaneous influence of formation temperature and pressure, (7) difficulties with the measurements of coefficient of linear thermal expansion at elevated temperatures (up to 250^{o}C) with measurements within every narrow temperature intervals (15-25^{o}C) that did not allow to determine a temperature dependence of the parameter.

A set of new equipment has been developed by us to remove these disadvantages and provide qualitatively new possibilities to get numerous reliable data on the thermal properties from the measurements on cores. Exploitation of these instruments has discovered new chances to test existing theoretical models, enhance these models and develop new theoretical models.

2. RESULTS

The new high effective methods and set of new instruments for thermal property measurements had been developed during last years that has improved essentially quality of the geothermal information as whole.

2.1 Optical Scanning Technique for Numerous Non-Destructive Non-Contact Measurements on Cores at Normal Conditions

The optical scanning method and instruments have been developed for non-contact measurements of thermal conductivity, and thermal diffusivity of rocks and minerals.

Optical scanning principle is a relatively new approach to thermo-physical measurements. A series of theoretical and experimental investigations was carried out by us to

evaluate its potential, and prototype measuring units were constructed (Popov et al., 1997; Popov et al., 1999). The theoretical model of the Optical Scanning Method (OS) is based on scanning a sample surface with three temperature sensors 1, 2 and 3 in combination with a focused, mobile and continuously operated constant heat source (Figure 1). The heat source and sensors move with the same speed *v* relative to the sample and at a constant distance to each other. Temperature sensor 1 displays the value of unheated sample surface temperature Θ_1 to take preliminary temperatures of the solids into account. Sensors 2 and 3 display the values of the rise of corresponding maximum temperatures Θ_2, and Θ_3 along the heating line behind the source.

Quasi-stationary excessive temperature rise, θ_2 -θ_1, in a moving coordinate system is determined by the relationship

$$\theta_2 - \theta_1 = \frac{Q}{2\pi \cdot x \cdot \lambda}, \quad (1)$$

where *Q* is the source power and *x* is the distance between the source and sensor 2.

If the samples under study and two reference standards with known conductivities λ_{R1} and λ_{R2} and thermal diffusivities correspondingly a_1 and a_2 are aligned along the scanning direction, the thermal conductivity of each sample can be determined from λ_R value and the ratio of (Θ_2-Θ_1) to (Θ_{2R}-Θ_{1R}) (for any reference standard R_1 or R_2) or, in actual application, from the ratio of electric signals (U_2-U_1) to (U_{2R}-U_{1R}), which are proportional to (Θ_2-Θ_1) to (Θ_{2R}-Θ_{1R}) values:

$$\lambda = \lambda R(\Theta 2R - \Theta 1R)(\Theta 2 - \Theta 1) - 1$$
$$= \lambda R(U2R - U1R)(U2 - U1) - 1 \quad (2)$$

For an anisotropic solid, the maximum temperature rise for sensor 2 is determined by the relationship (Popov et al., 1999)

$$\Theta = \frac{Q}{2\pi \cdot x \cdot \sqrt{\lambda_A \cdot \lambda_B \cdot \cos^2(\gamma') + \lambda_A \cdot \lambda_C \cdot \cos^2(\beta') + \lambda_B \cdot \lambda_C \cdot \cos^2(\alpha')}} \quad (3)$$

where Θ is sample excessive temperature, α', β' and γ' are angles between the A, B and C principal axes of thermal conductivity and the scanning line.

After scanning along three non-collinear and non-coplanar directions which are located on two non-parallel planes, equations (2) and (3) provide a means of determining the principal values of thermal conductivity from a set of three equations with three unknowns. For a sample with two-dimensional anisotropy, the principal values of conductivity can be determined from two non-collinear scans on one face, if this face is not parallel to the foliation.

Thermal diffusivity value of the samples under study can be determined using a following equation (Popov, 1997):

$$a = \frac{a_{R1} \cdot \ln\left(\frac{\lambda_{R1} \cdot \Theta_{R1}}{\lambda_{R2} \cdot \Theta_{R2}}\right)}{\ln\left(\frac{\lambda_{R1} \cdot \Theta_{R1}}{\lambda_{R2} \cdot \Theta_{R2}}\right) + \frac{a_{R2} - a_{R1}}{a_{R2}} \cdot \ln\left(\frac{\lambda \cdot \Theta}{\lambda_{R1} \cdot \Theta_{R1}}\right)} \quad (4)$$

Optical scanning allowed us to record the variations of thermal conductivity and diffusivity along the inhomogeneous sample and determine thermal conductivity and diffusivity tensor components for three-dimensional anisotropy. The other merits of optical scanning include (1) high precision (1.5%) and accuracy (1.5% for a confidence probability of 0.95) of thermal conductivity measurements within the range of 0.1-70.0 $W \cdot m^{-1} \cdot K^{-1}$, (2) high precision (2%) and accuracy (2%) of thermal diffusivity measurements within the range of $(0.1\text{-}5.0) \cdot 10^{-6}$ $m^2/s \cdot K$, (3) the ability to sample deeply using a slow scanning rate, (4) freedom from constraints for sample size (within 1 cm up to 70 cm in sample length) and shape and quality of mechanical treatment of the sample surface, (5) a contactless mode of measurements, (6) short time of measurement (10–30 s) for every sample, (7) the ability to measure on a flat or cylindrical sample surface, and (8) the possibility to measure on full cores and core plugs.

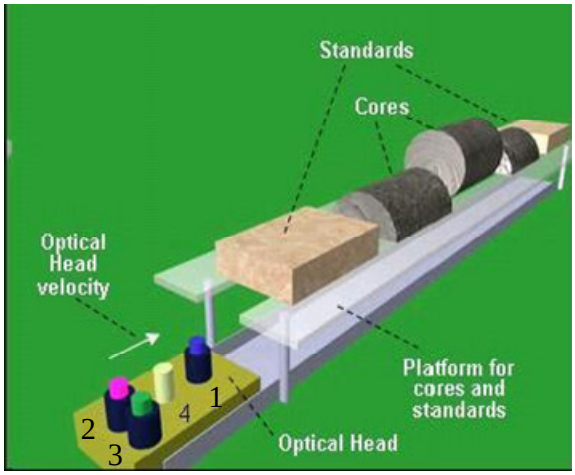

Figure 1: Scheme of a field version of the optical scanning instrument.

Two versions of optical scanning instruments have been elaborated: (1) the laser version for the measurements on core plugs and small pieces of rocks (from 1x1x1 cm and larger), and (2) the field version for numerous measurements on full cores in laboratory and core storages (Figure2). Both versions elaborated provide simultaneous measurement of thermal diffusivity as well as conductivity. The laser (or focused electric bulb) heat source and infrared radiometers for measurements of initial and maximum sample temperatures placed on a platform move at a constant speed relative to samples and reference standards. Measurements are carried out on dry or fluid-saturated samples. In the case of cylindrical samples, scans are oriented along the core axis and the bottom face of the core. Surface roughness of up to 1.0 mm is allowable. In general, it is not necessary to polish a sample surface. If the scanned surface is too rough systematic errors can be corrected based on results from reference standards with a similarly rough surface. The working surface of the sample is covered with an optical coating (25-40 μrn thick) in order to minimize the influence of varying optical reflection coefficients. Sample sizes in this study varied 1-70 cm in length, 2-30 cm in width, and 2 and more centimeters in thickness.

The specific feature of OS is the ability to change the thickness of the investigated surface-layer depending on the sample size and research goals. This can be done by a change in measurement regime including the speed of

scanning and the distance between the heated spot and the area of temperature recording. The layer thickness also depends on the thermal properties of the sample and may reach 2-3 cm or more for samples with thermal conductivity exceeding 6-7 $W \cdot m^{-1} \cdot K^{-1}$.

Figure 2: Optical scanning instrument for rock thermal property measurements on full cores.

The signal-processing algorithm yields the effective conductivity of two perpendicular directions for an inhomogeneous layered sample. The mean level of excessive temperature value along the scanning profile is used in eq. (2) for the determination of thermal conductivity in the orientation coincident with the scanning direction, and the thermal conductivity normal to the heated surface is determined as an arithmetic mean of local conductivities along the entire scanning line. Experimental studies of inhomogeneous samples consisting of up to 20 layers with thermal conductivities ranging from 1.35 to 21.0 $W \cdot m^{-1} \cdot K^{-1}$ and thicknesses varying from 1 to 15 mm have shown that this determination of effective thermal conductivity does not differ significantly from the calculated thermal conductivity of layered samples. Local thermal conductivities and thermal diffusivities can be determined for grain scales as small as 7 to 10 mm.

After the scanning is completed, the following information is available for each sample:

- thermal conductivity and thermal diffusivity profiles along a single scanning line,
- the effective thermal conductivity and thermal diffusivity of each sample for two mutually perpendicular directions and the related macro-anisotropy factor,
- the thermal inhomogeneity factor (defined as the maximum difference in conductivity along the scanning line divided by the effective thermal conductivity), and the RMS deviation of local thermal conductivity values along each scanning line.

At present, the measurable range of conductivity is 0.1 to 70 $W \cdot m^{-1} \cdot K^{-1}$. The rate of measurements is between 50 and 70 measurements per hour

The new methods and instruments described above have been used to perform measurements on the collections with more than 200 rock forming minerals (single crystals and aggregates) to correct and extend the data on thermal properties of minerals and their anisotropy and provide more reliable information for interpretation of rock thermal property variations. The new technologies have provided measurements on cores from deep wells with core sampling interval of 1-2 m. Significant vertical variations in rock thermal properties were established in every case not only for crystalline rocks but for sedimentary rocks also (the example of a thermal property log obtained on cores from a sandstone formation is given in Figure3). Our results of measurements on more than 80 000 cores from wells (including the scientific deep) drilled in different geological structures including geothermal energy fields have shown that rock's thermal conductivity correlates well with reservoir properties and is essentially anisotropic in most cases and varies in rock formations significantly (often by several times) even within cores and short depth intervals (several meters) in formations.

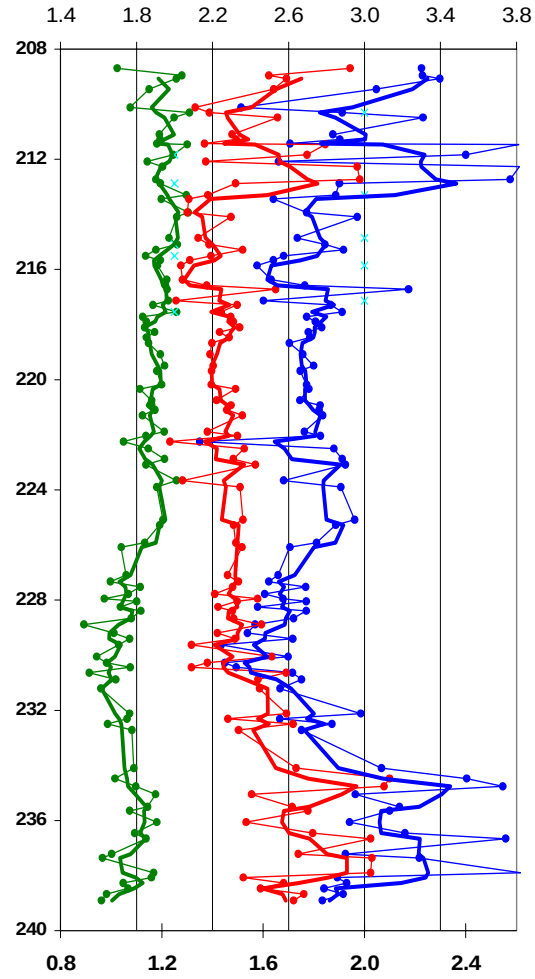

Figure 3: Thermal conductivity (blue points and line), thermal diffusivity (red color) and volumetric heat capacity (green color) logs from the optical scanning measurements on cores from sandstone-siltstone formation. Point represent original measurement data, thick lines correspond to the data from the filtering (box with 4 points), and vertical straight lines show mean values of the thermal properties within different depth intervals restricted by statistical boundaries found.

Vast new information about correlations between thermal and other physical properties (porosity, permeability, sonic velocity, electric resistivity) have been obtained from the measurements on more than 5000 core plugs of different sedimentary rocks due to possibility to measure many different physical properties on the same sample that reduced or excluded the rock inhomogeneity influence. Close correlations between thermal conductivity and porosity Φ of reservoirs are very stable and the correlations between permeability and relative change $\delta\lambda=\lambda_{dry}/\lambda_{sat}$ in thermal conductivity after water-saturation of rock samples

(λ_{dry} is thermal conductivity of dry rock samples and λ_{sat} is thermal conductivity of water-saturated rock samples) was established also (Figure 4).

2.2. Instrument for Measurements of Thermal Properties of Rocks and Minerals at Formation Pressure and Temperature

An instrument for measurements of rock's and mineral's thermal conductivity (TC) and thermal diffusivity (TD) with simultaneous influence of temperature (up to 250°C), and pore and two components of lithostatic pressures (up to 200 MPa) has been developed. The measuring pressure-temperature chamber of the instrument is shown in Figure5. A new approach in line-source method has been found to provide simultaneous measurements of TC and TD tensor components within one measurement cycle (Figure 6).

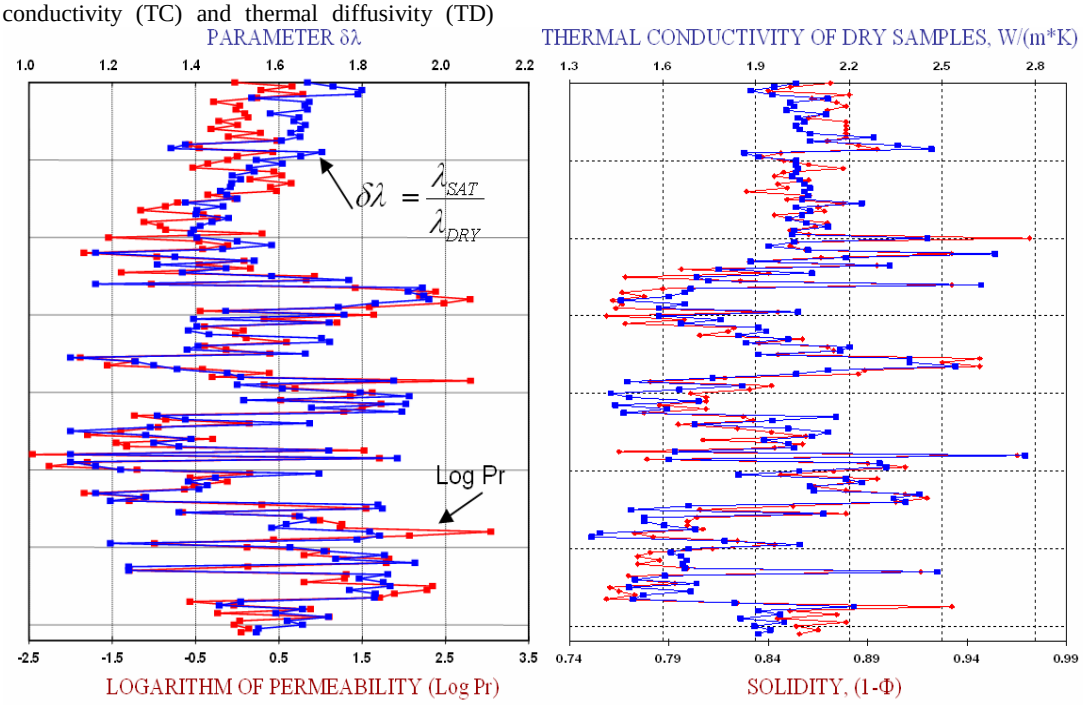

Figure 4: Logs of parameter $\delta\lambda=\lambda_{dry}/\lambda_{sat}$ (blue line) and logarithm of permeability Log P (red line) (left panel "a") and thermal conductivity λ_{dry} and solidity 1-Φ (Φ is porosity) (right panel "b"). Accuracy and precision of thermal conductivity measurements are 1.5% each (confidence probability of 0.95).

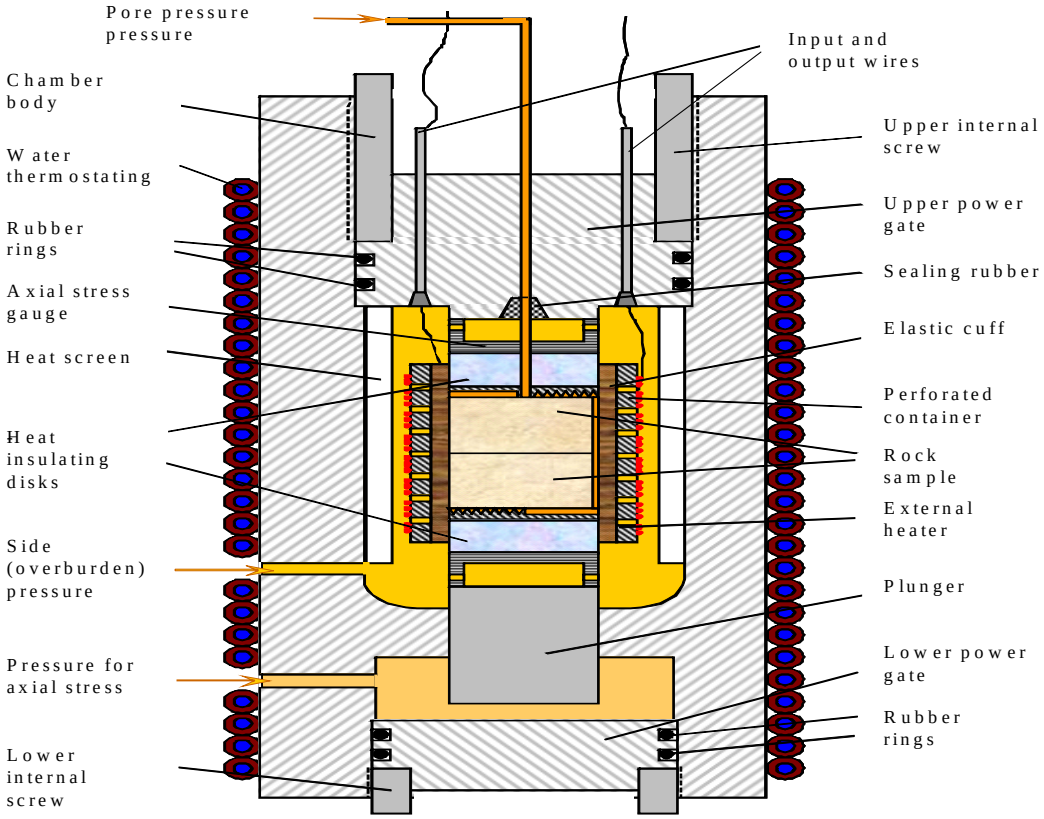

Figure 5: Scheme of chamber for thermal conductivity measurements at simultaneous acting elevated temperature, pore and two components of confining pressure.

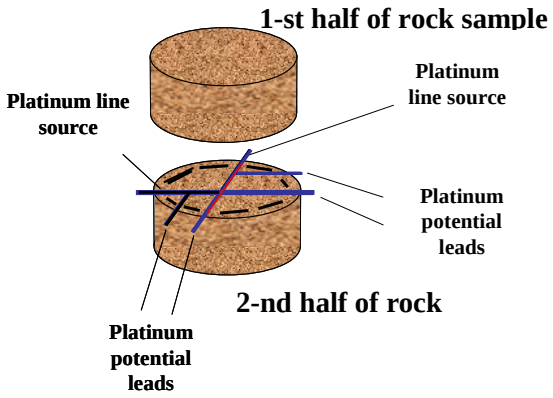

Figure 6: Measuring cell elaborated for simultaneous measurements of TC and TD tensor components at elevated *PT* conditions.

Comprehensive metrological studying the instruments designed for TC and TD measurements at simultaneous influence of elevated pressure P and temperature T within pressure range up to 250 MPa and temperature range up to 300 K is very complicated problem as no reliable references exist now and Standard Bureaus could not help to solve the problem at present. In our case the instrument metrological testing has been performed on set of 6 reference samples (glasses studied in industrial thermal physics) and a quartz single crystal with TC and TD values within ranges of respectively 0.71-10.7 $W \cdot m^{-1} \cdot K^{-1}$ and $(0.557\text{-}5.42) \cdot 10^{-6}$ m^2/s at simultaneous influence of elevated temperature and pressure.Natural quartz single crystal has been used also as a reference of anisotropy of thermal conductivity and thermal diffusivity. From the previous study of quartz single crystals of different natural types it was established that thermal properties of quartz single crystals are stable independently on their origination (Beck, 1977 and 1987; Popov et al, 1987, 1999). Quartz TC values were found from the consistent experimental data at room temperature determined by Beck (1987) (6.07±0.10 Wm-1 K^{-1} for the A and B axes and 10.5±0.1 $W \cdot m^{-1}$ K^{-1} for C axis) and Popov et al. (1987, 1999) (6.05±0.05 Wm^{-1} K^{-1} for A and B axes and 10.7±0.1 Wm^{-1} K^{-1} for C axis).

Thermal conductivity of the quartz single crystal was measured with the new apparatus with the line sources oriented in two directions relatively to the principal optical axes (C and A, B) of the crystal. The quartz crystal has hexagonal singony, therefore when the line source is oriented along the principal crystallographic axis *C* the thermal conductivity tensor components λ_a and λ_b ($\lambda_a = \lambda_b = \lambda_{a,b}$) are measured directly. When the line source is oriented perpendicularly to the *C* axis the apparent value of thermal conductivity λ^* measured is determined as $\lambda^* = \sqrt{\lambda_{a,b} \cdot \lambda_c}$ (Popov et al., 1999). The TC tensor component λ_c can be determined from these two measurements. The measurements on quartz single crystal allowed to test applicability of the instrument developed for measurements of thermal conductivity and thermal diffusivity tensor components on one rock sample. The TC&TD tensor components values measured with the new PT instrument at normal conditions simultaneously with two line sources, oriented perpendicularly each to other, were found to be $\lambda_{a,b}$ = 5.98 $W \cdot m^{-1} \cdot K^{-1}$ in the direction perpendicular to the main optical axis *C* and λ_c = 10.5 $W \cdot m^{-1} \cdot K^{-1}$ in parallel direction that corresponds satisfactorily to the TC values established earlier and mentioned above (Beck, 1987; Popov et al., 1987). As for TD values, they have been found to be equal to $a_{a,b} = 2.97 \cdot 10^{-6}$ m^2/s and $a_c = 5.18 \cdot 10^{-6}$ m^2/s. Results of simultaneous measurements of TC

tensor components at normal thermodynamical conditions and at elevated temperature (up to 130°C) and confining pressure (up to 130 MPa) compared with experimental data reported by Beck et al (1977) are presented in Figure 7. From the comparison of the new and published (Beck, 1977) experimental data for elevated PT conditions one can conclude that these TC values coincide well (within both measurement errors).

The performed metrological study described above demonstrate that the reliability of the new instrument designed is not interior to previous analogical instruments described in literature in respect to carefulness of metrological studying.

From testing the instrument on quartz single crystal at simultaneous influence of elevated temperature and pressure, total accuracy + precision value of thermal conductivity and thermal diffusivity measurements has been established to be correspondingly 4 and 7% (at confidence probability of 0.95).

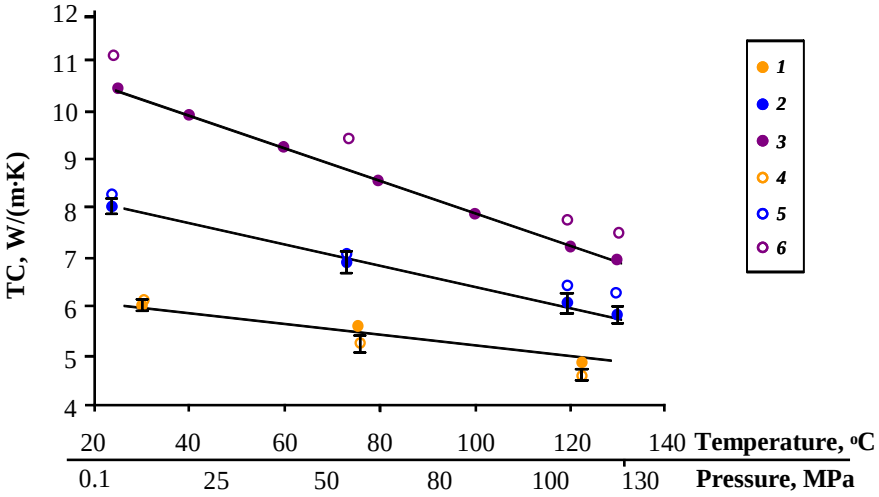

Figure 7: Comparison of TC tensor components $\lambda_{a,b}$ – (*1*, *4*), λ_c – (*3*, *6*) and $\lambda_{app} = \sqrt{\lambda_{a,b}\lambda_c}$ – (*2*, *5*), measured by: *1*, *2*, *3* – RSGPU and *4*, *5*, *6* – by Beck et al. (1977).

Behavior of TC and TD tensor components of quartz, calcite and potassium feldspar single crystals have been registered at simultaneous influence of temperature (up to 220°C) and confining pressure (up to 200 MPa). Analysis of experimental data and comparison with literature data have revealed that average difference in their values (1) does not exceed 5% for quartz, and (2) increases systematically up to 12% with the pressure and temperature increase for calcite and potassium feldspar single crystals.

Totally 223 sedimentary and crystalline rock samples (with porosity ranged respectively 0.2-37 and 0.1-3%) from Kamchatka peninsula, Chesapeake impact structure (USA), Ural superdeep well SG-4 (Russia) and territory of Germany have been studied at simultaneous influence of temperature and pressure. According to the measurement results for *sedimentary rocks* at elevated temperature 25-220°C and equal vertical and horizontal components of lithostatic pressure (up to 200 MPa) and pore pressure (up to 80 MPa), the thermal conductivity and thermal diffusivity decrease at pressure of 180 MPa and temperature of 120°C by -9−(-46)% and (-14)−(-64%) respectively.

Results of thermal property measurements on *crystalline rocks* at elevated temperature 25-120°C and equal vertical and horizontal components of lithostatic pressure have shown that thermal conductivity and thermal diffusivity vary at pressure of 170 MPa and temperature of 120°C by -6-(-26) % and -11-(-33)% respectively.

2.3. Pore Space Characterization

Combination of experimental thermal property data with a new theoretical model of effective thermal conductivity (λ_{eff}) of inhomogeneous porous rocks constructed on a self-consistent effective medium theory base has been used for estimation of pore/crack space geometry. In the model an each pore is assumed to be of elliptical shape (general ellipsoid) embedded in a medium having thermal conductivity $\lambda^{(0)}$ (Popov et al., 2004). The model formula for calculation of the effective thermal conductivity is as follows:

$$\lambda_{eff} = \left\langle \sum_{j=1}^{N} \phi_j \lambda^{(j)} \int P(F^{(j)};\theta,\varphi,\psi)\left[\lambda^{(0)}(I-F^{(j)})+\lambda^{(j)}F^{(j)}\right]^{-1} dF^{(j)} d\theta d\varphi d\psi \right\rangle^{-1} \times \left\langle \sum_{j=1}^{N} \phi_j \int P(F^{(j)};\theta,\varphi,\psi)\left[\lambda^{(0)}(I-F^{(j)})+\lambda^{(j)}F^{(j)}\right]^{-1} dF^{(j)} d\theta d\varphi d\psi \right\rangle^{-1} \quad (5)$$

Here I is the 4-th rank unit tensor; $F^{(j)}$ is the depolarization tensor depending on the ellipsoid shape and matrix properties; θ, φ and ψ are the Eulerian angles specifying the rotation of inclusions in space, ϕ_j, $P(F^{(j)}; \theta, \varphi, \psi)$ are volume concentration and distribution function over shape and orientation of the j-th component, and N is the number of components.

If the effective thermal conductivity values are determined from the measurements on dry (λ_{dry}) and fluid-saturated (λ_{sat}) rock sample and porosity Φ is known, an average value of the pore aspect ratio α can be calculated from a set of two equations based on (5) (Popov et al., 2004):

$$\begin{cases} \lambda_{eff}\left(\Phi, \alpha, \lambda_m, \lambda_{air}\right) = \lambda_{dry} \\ \lambda_{eff}\left(\Phi, \alpha, \lambda_m, \lambda_{water}\right) = \lambda_{sat} \end{cases} \quad (6)$$

Thermal conductivity of air λ_{air} is 0.024 $W \cdot m^{-1} \cdot K^{-1}$ and water λ_{water} is 0.60 $W \cdot m^{-1} \cdot K^{-1}$ (Vargaftik, 1990). It follows

from (6) that the rock matrix conductivity λ_m and the aspect ratio α of cracks can be assessed. The set of non-linear equations (6) can be solved numerically using the procedure of non-linear optimization.

The procedure of aspect ratio estimation is applied in combination with numerous measurements of the thermal properties on cores that allow us to differentiate rock formations in pore space geometry parameters (Popov et al., 2003, 2004).

Rock matrix thermal conductivity can be estimated also from the simple Lichtenecker's theoretical model that improves the reliability of the procedure described above. The Lichtenecker's model is being used often for thermal conductivity prediction also (Schoen, 1996). A simple engineering Assad's modification of the Lichtenecker's theoretical model has been recommended to estimate effective thermal conductivity of rocks using known data on porosity and rock matrix thermal conductivity taking the pore space peculiarities into account (Assad, 1955):

$$\lambda_{eff} = \lambda_m^{(1-f\Phi)} \lambda_{fluid}^{f\Phi} \tag{7}$$

where f is a correction factor.

Nevertheless, the correction factor f values were not estimated earlier. If the rock matrix thermal conductivity is estimated from the thermal conductivity versus porosity plot, correction factor f value can be calculated from (7) as follows:

$$f = Ln\left(\frac{\lambda_m}{\lambda_{eff}}\right) \Big/ \left(\Phi Ln\left(\frac{\lambda_m}{\lambda_{fluid}}\right)\right) \tag{8}$$

Our numerous measurements on core collections with different rock types allowed us to obtain the representative data on correction factor from the (4). From these measurements it was established that the correction factor f depends on rock type, a degree of sedimentation, pore space geometry and fluid type in pores and varies in range of 0.35-1.70.

2.4. New Technique for Fluid Thermal Conductivity Measurements at Elevated Temperatures

A new technique for thermal conductivity measurements based on the line-source theoretical model has been developed. A measuring needle probe consists of a platinum heater and potential taps for temperature recording.

A main advantage of the developed technique is that an operator can manually choose time interval for experimental data processing from an observation of signal temporal variations (Figure 8). Thus the disturbing effect of fluid natural convection can be excluded from the measurement results.

For measurements of fluid TC at elevated temperature the developed needle probe is installed vertically into a high temperature cell for natural convection effect reduction (compared to a horizontal position) and placed into a programming high temperature furnace.

Metrological testing of the developed technique has been performed. The distilled water and glycerin were used as reference fluids for testing since dependencies thermal conductivity versus temperature are well known for these fluids (Vargaftik, 1990). The metrological testing results and the reference data are given in Figures 9 and 10 for a temperature range of 0–160°C.

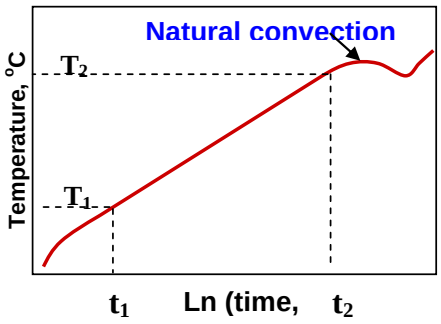

Figure 8: Temperature vs time plot demonstrating thermal convection effect which can disturb the measurement results.

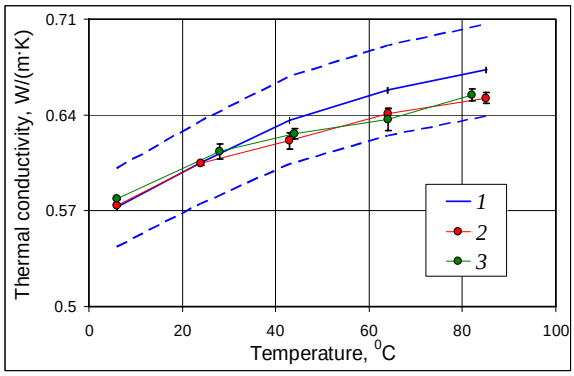

Figure 9: Comparison of measured thermal conductivity of water with the reference data: *1* – reference data, *2* – 1st cycle of measurements, *3* – 2nd cycle of measurements. Bars on the experimental data are the RMS values. Dashed blue lines are the ±5% values of reference data.

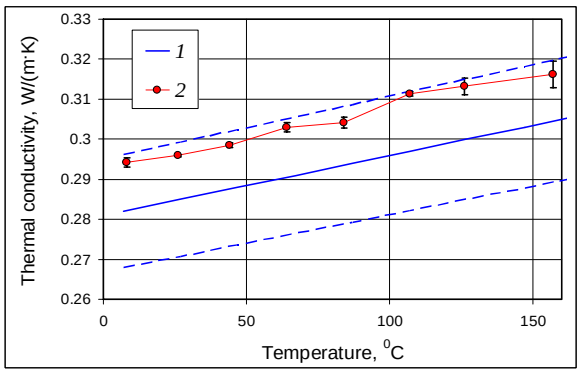

Figure 10: Comparison of measured thermal conductivity of glycerin with the reference data: *1* – reference data, *2* – experimental data. Bars on the experimental data are the RMS values. Dashed blue lines are the ±5% values of reference data.

Estimated precision is ± 3.5% at confidence of probability 0.95 and systematic deviation does not exceed 5%. It was established from the metrological testing that a lower bound of the fluid viscosity range where the accurate measurements can be done with the quality mentioned above is $3 \cdot 10^{-4}$ Pa·s.

2.4. Instrument for Measurements of Linear Thermal Expansion Coefficient of Rocks

The quartz dilatometer for the measurements of the coefficient of linear thermal expansion (CLTE) of rock and mineral samples has been elaborated. The instrument provides the CLTE measurements on crystals of rock forming minerals and core plugs (cylinders with diameter of 30 mm and height of 30 mm) which are being used in petrophysics for measurements of many physical properties. The instrument allows us also to measure the CLTE on cubes with a side of 30 mm. It provides the reliable data on CLTE anisotropy when we measure the CLTE in three cube positions. Such measurement technique excludes the inhomoheneity influence that can not be allowed if we study the CLTE anisotropy on three samples prepared from one rock samples along three perpendicular directions as it recommended usually.

Numerical modeling temperature field within a sample volume during its heating and cooling under the CLTE measurements allowed us to estimate temperature gradients within the sample depending on sample dimensions and thermal properties and rate of heating and cooling to reach better measurement quality. It allowed also. To test the numerical model results the experiments have been performed when thermocouples were placed into the sample and on its surface. It was established from the theoretical and experimental results that rate of sample cooling and heating should not be larger than 1 K/min and temperature gradient within the sample should not be larger than 0.5 K/cm.

The instrument provides the CLTE measurements for every temperature interval of 20 ^{0}C that allows us to establish a regularity in the CLTE variations within the temperature range of 20-250^{o}C with a temperature step of 20^{o}C. A total relative accuracy + precision (at a confidence probability of 0.95) for every 20^{o}C interval was established from the metrological experiments to be not more than ±4%.

Metrological testing the CLTE instrument developed has been performed on the certificated reference standards (fused quartz, silicon single crystal, cuprum, aluminium) with the CLTE values within the range of $(0.5\text{-}24.6)\cdot10^{-6}$ K^{-1}, that covers in general a range of rock and mineral CLTE values $(2.5\text{-}18)\cdot10^{-6}$ K^{-1}.

The measurements on a quartz crystal have shown that the discrepancy is observed between previous and experimental data on the quartz CLTE. Our new data obtained from the new instrument application exceed by 20% the previous data (Clark 1966; Raz et al., 2002).

The CLTE instrument has been used for regular measurements on core collections for carbonate rocks from oil-gas fields in the West Siberia (Russia). A small precision and possibility to determine the CLTE value for every 20^{0}C temperature interval allowed to establish the CLTE vs temperature dependence within a temperature interval of 20−100^{o}C which was chosen to prevent a rock sample destruction. The CLTE values were found to range $(3.48\text{-}10.8)\cdot10^{-6}$ K^{-1} at 30^{o}C and $(4.50\text{-}14.4)\cdot10^{-6}$ K^{-1} at 100^{o}C

3. CONCLUSIONS

1. The technique and instruments developed provide the measurements of vast set of the rock thermal properties and allow to improve experimental thermal property data of formations.

2. The optical scanning technology provides high precision of measurements, high speed of operation, contactless mode of measurement, the ability to measure directly on full cores and core plugs without mechanical treatment with simultaneous determination of thermal conductivity and thermal diffusivity, thermal anisotropy and estimation of inhomogeneity of rocks.

3. The optical scanning technology application reveals a possibility to study correlations of thermal properties with other physical properties from the measurements on the same core plugs that reduces a disturbing influence of rock inhomogeneity and anisotropy and allows to establish more reliable correlations between the properties.

4. Essential thermal inhomogenity of rock formations discovered from the numerous optical scanning measurements demonstrate necessity of the measurements on representative core collections with detailed core sampling along wells.

5. The new instrument for the rock thermal property measurements at formation conditions allows to determine simultaneously the thermal conductivity and diffusivity tensor components at simultaneous influence of elevated temperature and three component pressure (pore, axial and confining pressure components).

6. The instrument developed for fluid thermal conductivity measurements provides the measurements for fluids with wide range of viscosity without disturbing influence of thermal convection in low viscous fluids.

7. The instrument developed for the coefficient of linear thermal expansion provide measurements the coefficient tensor components on one sample within the temperature range of 20−250^{o}C with a temperature step of 20^{o}C.

ACKNOWLEDGMENTS

The authors would like to acknowledge the generous support of Schlumberger Oilfield Services, the international company in oil-gas industry, and Russian Foundation for Basic Research (grants 00-05-72021 and 08-05-00977).

REFERENCES

Assad Y.: A study of the thermal conductivity of fluid bearing porous rocks, *PhD Dissertation*, Univ. of Calif., Berkeley, (1955), 71 p.

Beck A.E., Darbha D.M., and Schloessin H.H.: Lattice conductivities of single-crystal and polycrystalline materials at mantle pressure and temperatures, *Phys. Earth Planet. Inter.***, 17**, (1977), 35–53.

Beck A.E.: Methods for determining thermal conductivity and thermal diffusivity. In : *Handbook on Terrestrial Heat Flow Density Determination*, Ed. by Haenel, Rybach and Stegena, Kluwer, Dordrecht, (1987), 87-124.

Burkhardt, H., Honarmund. H., Pribnow, D.:First results of thermal conductivity measurements with a borehole tool for great depths. In: Bram. Draxler, Kessels, Zoth, (Eds.). *KTB Report*, 9(6a). Springer Verlag. Hannover, (1990). 245-258.

Clark, J., S.P.: *Handbook of Physical Constants* Yale University, New Haven, Connecticut, 544 p, (1966)

Kukkonen I., Suppala I., Korpisalo A. and Koshkinen T. Drill hole logging device TERO76 for determination of rock thermal properties, *Posiva 2007-01*, Geological Survey of Finland, Posiva OY, (2007), p.63.

Popov Yu., Romushkevich R., Bayuk I., Korobkov D., Mayr S., Burkhardt H., and Wilhelm H.: Physical properties of rocks from the upper part of the Yaxcopoil-1 drill hole, Chicxulub crater, *Meteoritics & Planetary Science*, **39 (6)**, (2004), 799-812.

Popov Yu., Tertychnyi V., Romushkevich R., Korobkov D., and Pohl J.: Interrelations between thermal conductivity and other physical properties of rocks: experimental data, *Pure and Appl. Geophys.*, **160**, (2003), 1137-1161.

Popov Yu.: Optical scanning technology for nondestructive contactless measurements of thermal conductivity and diffusivity of solid matters, *Proceedings*, 4th World Conf. Experimental Heat Transfer, Fluid Mechanics and Thermodynamics, Brussels, **1**, (1997), 109-117.

Popov Yu.A., Berezin V.V., Soloviov G.A., Romuschkevitch R.A., Korosteliov V.M., Kostiurin A.A., and Kulikov A.V.: Thermal conductivity of minerals, *Izvestiya Physics of the Solid Earth*, **23 (3)**, (1987), 245-253.

Popov Yu.A., Pribnow D., Sass J., Williams C., and Burkhardt H.: Characterisation of rock thermal conductivity by high-resolution optical scanning, *Geothermics*, **28**, (1999), 253-276.

Pribnow, D., Williams, C, Burkhardt, H.: Log-derived estimate for thermal conductivity of crystalline rocks from the 4 km KTB. Vorbohrung. *Geophysical Research Letters*, 20, (1993), 1155-1158.

Raz, U., Girsperger, S. and Thompson, A.: *Thermal expansion, compressibility and volumetric changes of quartz obtained by single crystal dilatometry to 700°C and 3.5 kilobars (0.35 GPa).* ETH, Eidgenössische Technische Hochschule Zürich, Department of Earth Sciences, Zürich, 73 p, (2002)

Schoen, J.H.: Physical properties of rocks: fundamentals and principles of petrophysics Handbook of geophysical exploration, Section I, *Seismic exploration*, **18**, Redwood Books, Trowbridge, (1996), 468 p.

Vargaftik N.B., Filippov L.P., Tarzimanov A.A. and TotskiyE.E.: Thermal conductivity of fluids and gases, *Handbook*, Moscow, Energoatomizdat, (1990), 352 p. (in Russian).

Wilhelm, H.: A new approach to the borehole temperature relaxation method, *Geophysical Journal International*, **103**, (1990), 469-481.

Williams, C.F., and Anderson, R.N.: Thermophysical properties of the Earth's crust: *in situ* measurements from continental and ocean drilling, *Journal of Geophysical Research*, **95**, (1990), 9209-9236.